Near-Surface Temperature Lapse Rates over Arctic Glaciers and Their Implications for Temperature Downscaling

ALEX S. GARDNER,* MARTIN J. SHARP,* ROY M. KOERNER,[+],[#] CLAUDE LABINE,*,[@]
SARAH BOON,*,[&] SHAWN J. MARSHALL,** DAVID O. BURGESS,*,[++] AND DAVID LEWIS*

* Department of Earth and Atmospheric Sciences, University of Alberta, Edmonton, Alberta, Canada
[+] Geological Survey of Canada, Ottawa, Ontario, Canada
[@] Campbell Scientific (Canada) Limited, Edmonton, Alberta, Canada
[&] Department of Geography, University of Lethbridge, Lethbridge, Alberta, Canada
** Department of Geography, University of Calgary, Calgary, Alberta, Canada
[++] Canada Centre for Remote Sensing, Natural Resources Canada, Ottawa, Ontario, Canada

ABSTRACT

Distributed glacier surface melt models are often forced using air temperature fields that are either downscaled from climate models or reanalysis, or extrapolated from station measurements. Typically, the downscaling and/or extrapolation are performed using a constant temperature lapse rate, which is often taken to be the free-air moist adiabatic lapse rate (MALR: $6°–7°C\,km^{-1}$). To explore the validity of this approach, the authors examined altitudinal gradients in daily mean air temperature along six transects across four glaciers in the Canadian high Arctic. The dataset includes over 58 000 daily averaged temperature measurements from 69 sensors covering the period 1988–2007. Temperature lapse rates near glacier surfaces vary on both daily and seasonal time scales, are consistently lower than the MALR (ablation season mean: $4.9°C\,km^{-1}$), and exhibit strong regional covariance. A significant fraction of the daily variability in lapse rates is associated with changes in free-atmospheric temperatures (higher temperatures = lower lapse rates). The temperature fields generated by downscaling point location summit elevation temperatures to the glacier surface using temporally variable lapse rates are a substantial improvement over those generated using the static MALR. These findings suggest that lower near-surface temperature lapse rates can be expected under a warming climate and that the air temperature near the glacier surface is less sensitive to changes in the temperature of the free atmosphere than is generally assumed.

1. Introduction

Mass loss from glaciers and ice caps is likely the second largest contribution to global sea level rise after ocean thermal expansion (Meier et al. 2007). Quantifying past contributions from this source is challenging because of the limited availability of measurements of glacier surface mass balance and rates of iceberg calving. Glacier surface mass balance models are widely used to compensate for this lack of measurements and can be used to predict how climate change will influence future glacier contributions to global eustatic sea level (Gregory and Oerlemans 1998; Braithwaite and Raper 2002; Marshall et al. 2005; Bougamont et al. 2005; Hanna et al. 2005).

Mass balance models calculate snow and ice melt using two main approaches: the energy balance approach and the temperature-index or "degree day" approach. The latter approach assumes an empirical relationship between melting and near-surface air temperature, while the former involves the assessment of all the major energy fluxes to and from the glacier surface in order to determine the energy available for melt. In either case, spatially distributed modeling is required to capture spatial and temporal patterns of surface melt (Glover 1999; Arnold et al. 2006). Such modeling requires accurate downscaling of coarse-resolution temperature fields derived from climate models or reanalysis to produce near-surface air

temperature fields with an appropriate spatial resolution. Downscaling can be performed either by running a regional climate model (forced at its boundaries with coarse-resolution climate model output or data from climate reanalysis) at the desired resolution or by computing near-surface temperatures from climate model fields using a digital elevation model of the glacier surface and an assumed temperature lapse rate.

"Lapse rate" is defined as "the decrease of an atmospheric variable with height, the variable being temperature, unless otherwise specified" (Glickman 2000), and it often refers to the environmental lapse rate in a vertical profile of the atmosphere. Here we use lapse rate to refer to the decrease in near-surface temperature with elevation following the glacier surface. We define lapse rates to be positive when temperature decreases as elevation increases in order to be consistent with usage in the atmospheric science community. However, we note that most previously published glacier near-surface lapse rates have been given the reverse sign convention (positive lapse rate = increase in temperature with increasing elevation; Braun and Hock 2004; Hanna et al. 2005; Otto-Bliesner et al. 2006b; Marshall et al. 2007; Gardner and Sharp 2009). This difference in sign convention should be noted when comparing our results with those presented in these other studies.

Regional climate modeling at high spatial resolution requires extensive computational resources, so this approach is best suited for downscaling temperature fields spanning short time periods to either relatively small ice masses or larger ice masses with low spatial gradients in melt rates. For large and complex regions like the Canadian high Arctic, running a regional climate model for multiple years at a resolution desirable for modeling glacier melt ($\sim$1 km) is computationally challenging, so statistical temperature downscaling remains an attractive proposition. The lapse rate used to downscale near-surface temperatures is often taken to be the moist adiabatic lapse rate (MALR = 6°–7°C km^{-1}; Glover 1999; Flowers and Clarke 2002; Thomas et al. 2003; Arnold et al. 2006; Bassford et al. 2006a,b; de Woul et al. 2006; Otto-Bliesner et al. 2006a; Raper and Braithwaite 2006). However, temperature lapse rates measured close to glacier surfaces can differ substantially from the MALR (Greuell and Böhm 1998; Braun and Hock 2004; Hanna et al. 2005; Marshall et al. 2007). Neglecting to account for these differences may result in large errors in downscaled temperature fields and in the magnitude and spatial distribution of modeled glacier melt (Greuell and Böhm 1998; Otto-Bliesner et al. 2006b; Gardner and Sharp 2009).

Near-surface temperature lapse rates vary on diurnal and seasonal time scales because of changes in the sensible heat flux between the free atmosphere and the underlying surface. This flux is influenced by temporal and spatial changes in free-atmosphere and surface temperatures, surface roughness, and wind speed. Because near-surface air temperatures are intermediate between those of the free atmosphere and the surface and surface temperatures over a melting glacier are fixed at the melting point temperature, near-surface lapse rates over melting glaciers are often lower than lapse rates in the free atmosphere (Greuell and Böhm 1998). Marshall et al. (2007) found that measured near-surface lapse rates over a Canadian Arctic ice field were systematically lower than free-air lapse rates, and that daily changes in lapse rates were associated with changes in synoptic weather patterns. In the summer, lapse rates were closer to the free-air MALR when there was enhanced cyclonic activity, but were considerably lower than the MALR ($<$2°C km^{-1}) when anticyclonic circulation prevailed.

Here we discuss measurements of surface air temperatures and lapse rates made on four large ice masses in the Canadian high Arctic at various intervals during the period 1988–2007. The Canadian high Arctic contains the largest volume of land ice in the world outside Greenland and Antarctica and is a potentially significant contributor to global sea level change. Mass balance measurements have been made at five sites in the region for over 40 yr (Cogley et al. 1996; Koerner 2005), but little is known about the magnitude, trends, and interannual variability of glacier mass balance across much of the region. Distributed, regional-scale mass balance modeling is required to better estimate both past and future contributions of glacier melt in this region to global sea level change. The goals of this study are therefore (i) to determine whether the relationships identified by Marshall et al. (2007) apply throughout the region, (ii) to develop and validate an empirical method to model temporally variable lapse rates that can be used to downscale temperature fields derived from climate models or reanalysis to the complex surface topography of these ice masses, and (iii) to compare the results from this method with those generated by downscaling using the MALR.

Our analysis is based on six datasets from the Prince of Wales Ice Field, the Agassiz Ice Cap, the John Evans Glacier on Ellesmere Island, and the Devon Island Ice Cap (Fig. 1). These datasets contain over 58 000 measurements of daily mean temperature from 69 sensors covering the period June 1988 to May 2007. Near-surface lapse rates were calculated from these datasets and compared with estimates of daily mean lower-troposphere temperatures derived from the National Centers for Environmental Prediction's North American Regional Reanalysis
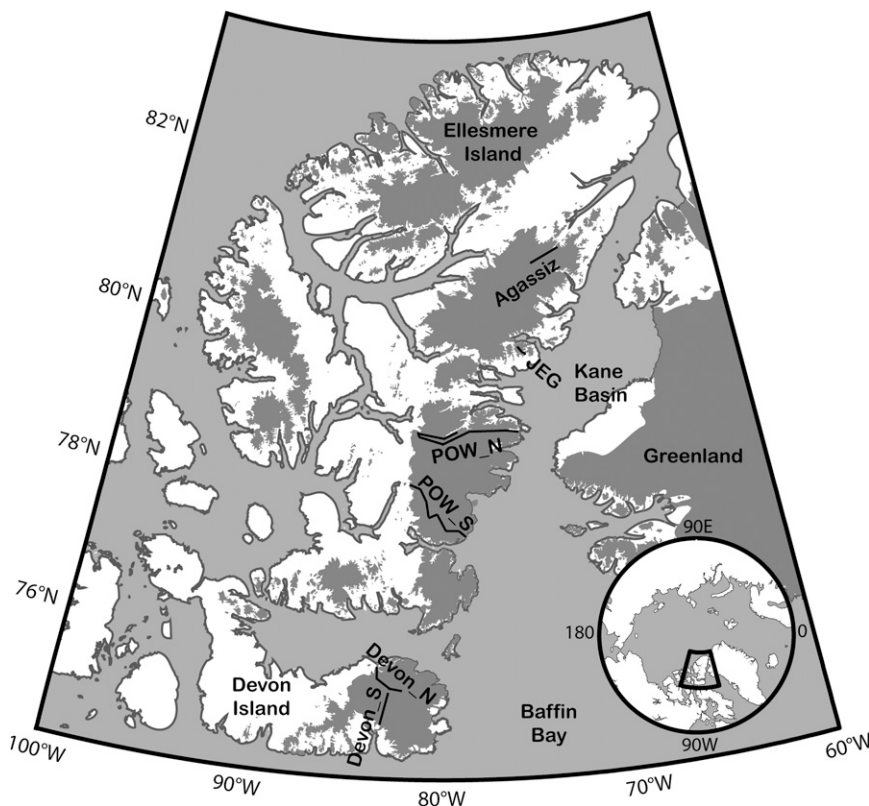
FIG. 1. Map of Canadian high Arctic with the six temperature–elevation sensor transects shown with heavy black lines.

(NARR; Mesinger et al. 2006). We present an empirical approach to downscaling the NARR temperatures that involves the prediction of near-surface lapse rates over glaciers from NARR 750-mbar mean daily air temperature standardized anomalies, where anomalies are taken relative to the 1979–2006 summer mean temperature and have been standardized by dividing the anomalies by their respective standard deviation. NARR bias-corrected summit elevation air temperatures were then downscaled using the modeled near-surface lapse rate for each day.

2. Site details

a. Agassiz Ice Cap

The 21 000 km^2 Agassiz Ice Cap, located on the eastern side of Ellesmere Island (Fig. 1), is the second largest ice cap in the Canadian high Arctic (Sharp et al. 2003). In the spring of 1988, an automatic weather station (A_1) was erected at the site where two surface-to-bedrock boreholes were drilled by the Geological Survey of Canada in 1984 and 1987 (Koerner and Fisher 1990; Fisher et al. 1995). Two more stations were installed at lower elevations along a northeast-oriented transect in

June 1991 (A_2) and April 1994 (A_3). All three stations are equipped with Campbell Scientific (CS) 107F temperature sensors. These stations are still in operation, are maintained annually by CS Canada Ltd. and the Geological Survey of Canada, and comprise the Agassiz transect, which extends 30 km horizontally and ranges in elevation from 880 to 1740 m MSL.

b. Devon Island Ice Cap

The dome-shaped Devon Island Ice Cap (area ~14 000 km^2) on the eastern side of Devon Island (Fig. 1) is the southernmost glacier included in this study. Two of the six temperature–elevation transects are located on this ice cap. The longest running transect, Devon_N, is located on the north slope of the ice cap and spans a horizontal distance of >40 km and an elevation range from 330 to 1880 m MSL. It consists of six automatic weather stations installed between 1992 and 2005, four of which are currently in operation and are maintained by the Geological Survey of Canada (Koerner 2005). All temperatures are measured with CS 107F sensors.

The second transect, Devon_S, is located on the south-facing slope of the ice cap and consists of three CS 107F

sensors and 17 HOBO H8-PRO sensors manufactured by Onset Scientific Ltd. Sensors were installed between 2004 and 2006 and were distributed at ~2 km intervals along a 50-km transect from the ice cap summit to its southern margin. Most sensors on this transect, which spans an elevation range from 480 to 1800 m MSL, are currently operational and are maintained by the Arctic and Alpine Research Group at the University of Alberta.

c. John Evans Glacier

John Evans Glacier, the only valley glacier included in this study, is located on the east coast of Ellesmere Island to the south of the Agassiz Ice Cap (Fig. 1). In June 1996, three HMP35CF relative humidity–temperature sensors were installed on automatic weather stations located at elevations of 260, 820, and 1180 m MSL (Arendt and Sharp 1999; Boon et al. 2003). In May 2001, 16 HOBO H8-PRO temperature sensors were installed at ~100-m vertical intervals along a 15-km transect [John Evans Glacier (JEG) transect] following the centerline of the glacier from its terminus (140 m) to its summit (1470 m). The weather stations and the 16 HOBO sensors were removed in June 2003.

d. Prince of Wales Ice Field

The Prince of Wales Ice Field is located in eastern Ellesmere Island, to the south of John Evans Glacier (Fig. 1). Two temperature–elevation sensor transects were operated on the ice field between 2001 and 2003 (Marshall et al. 2007). The 170-km Prince of Wales ice Field (POW)_N transect, which crosses the northern part of the ice field, was installed in spring 2001. It consisted of one CS 107, one Veriteq Instruments Inc. SP-2000, and 12 HOBO H8-PRO temperature sensors located at elevations ranging from 130 to 1730 m MSL. The 130-km southern transect, POW_S, which spanned an elevation range from 550 to 1350 m MSL, was installed in spring 2002 and consisted of two SP-2000 and four HOBO H8-PRO temperature sensors. All sensors were removed in spring 2003. Marshall et al. (2007) provide a more detailed description of the ice field and the datasets derived from these transects.

3. Data and methods

a. Near-surface temperatures

All temperature sensors were installed in solar radiation shields mounted on metal or plastic poles drilled into the glacier surface. Sensors were mounted between 1 and 1.5 m above the surface and in open locations representative of the surrounding area. Temperatures were originally recorded as 15 min, 30 min, 1 h, 2 h, or daily averages and were postprocessed to produce daily averages. A list of all temperature sensors used in the study, locations, and periods of operation can be found in the appendix (Table A1) along with sensor specifications (Table A2).

Sensor measurement accuracies range between ±1.0°C at low (<−30°C) temperatures and ±0.2°C at 0°C (Table A2). Marshall et al. (2007) conducted an extensive study to determine additional errors due to instrument calibration (0.1°–0.7°C) and varying sensor height relative to the glacier surface (±0.1°C for daily averages). They estimated the overall uncertainty in the daily average temperature measurements to be ±1.3°C. This value is also adopted for the measurement error in this study.

Gaps in sensor records exist (mostly during winter months) where stations were removed for servicing, because the battery or sensor failed, when sensors were found less than 0.5 m (high accumulation) or more than 2.5 m (high ablation) above the surface, and where sensor poles collapsed because of ablation or interference from polar bears. Figure 2a shows the annual number of daily averaged temperature measurements made along each transect. All quality controlled daily average temperature measurements for each transect have been included as supplementary material for this manuscript and can be found online at the University of Alberta Arctic and Alpine Research Group's Web site (http://arctic.eas.ualberta.ca/).

b. Lapse rates

Using daily mean temperatures and assuming constant sensor elevations, daily lapse rates were calculated for each transect using simple linear regression. For the Devon_S, JEG, POW_N, and POW_S transects, measured temperatures below −30°C were excluded from lapse rate calculations because of increased instrument errors at these temperatures. For the Agassiz and Devon_N transects, where CS 107F temperature sensors were used, all temperatures below −50°C were excluded. Lapse rates were only calculated when three or more separate temperature measurements were available along a transect, and when the elevation difference between the lowest and highest available stations exceeded 500 m. These criteria reduce the impact of temperature measurement errors on calculated lapse rates, but also reduce the number of days for which lapse rates can be calculated. For the six transects, between 44% and 91% of days with temperature measurements yielded lapse rates (Fig. 2b). There are fewer than 20 days of data for POW_S in January, February, and March, so no values are reported for these months and the POW_S transect is omitted from the discussion of winter lapse rates.
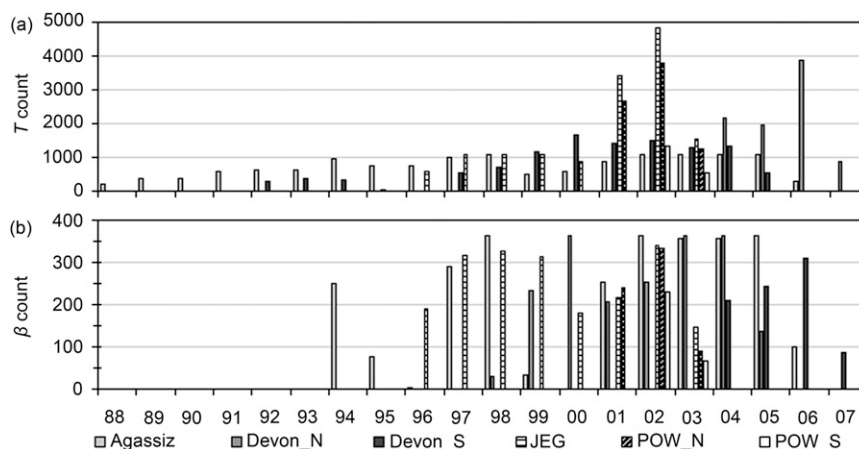
FIG. 2. Annual number of (a) daily averaged temperature measurements and (b) calculated lapse rates (β) for each of the six near-surface glacier temperature–elevation transects.

c. Regional climate reanalysis

The NARR dataset (32 km and 45 layer) is available for the period from 1979 to 2006 for the entire North American region. Data were provided by the National Oceanic and Atmospheric Administration/Office of Oceanic and Atmospheric Research/Earth System Research Laboratory (NOAA/OAR/ESRL) Physical Sciences Division (PSD), Boulder, Colorado, from their Web site (http://www.cdc.noaa.gov/).

The variables 500-mbar geopotential height (500Z) and 750-mbar air temperature (750T) were selected to characterize atmospheric conditions over the four Canadian high Arctic glaciers. Here 500Z was chosen to describe synoptic-scale variability in the midtroposphere, which has a strong influence on lower-troposphere temperatures, regional glacier melt, and near-surface lapse rates in the Canadian high Arctic (Alt 1987; Wang et al. 2005; Gardner and Sharp 2007; Marshall et al. 2007); 750T was selected to describe free-air temperatures at an elevation of ~2200 m MSL, which is at least 500 m above the NARR model topography in the regions of the four glaciers examined in this study. The influence of changes in free-atmospheric temperatures was investigated because these temperatures can affect near-surface lapse rates directly by modifying the sensible heat flux to and from the surface and indirectly by altering other surface energy balance components (i.e., the amount of absorbed solar radiation through melt-induced modification of the surface albedo). The influence of atmospheric winds was also investigated because winds can modify both free-air and near-surface lapse rates through the horizontal advection of air masses of different temperatures and moisture contents, by forcing the ascent/descent of advected air masses over terrain and by altering the

turbulent heat fluxes between the free atmosphere and the surface. However, no consistent relationships were found between wind components and lapse rates.

Daily average time series for the selected NARR variables were created for each glacier by averaging over a six-gridcell domain (96 km by 64 km) centered over each glacier. All time series were generated for the period January 1988 to December 2006, which extends from the first year of on-glacier temperature data to the last year of NARR data available from the NOAA/OAR/ESRL Physical Sciences Division's Web site.

To ensure that the NARR data accurately model climatic variability over the region of interest, 750T (averaged over the regions occupied by each glacier) was correlated with individual temperature series from on-glacier sensors located above 1000 m MSL on each glacier. All near-surface measurements are highly positively correlated with the corresponding NARR 750T (annual: $r = 0.84–0.98$; summer: $r = 0.71–0.92$). As with other correlations presented in this paper, monthly means were subtracted from the time series prior to correlation.

d. Statistical analysis

Pearson product–moment correlation analysis (Shumway and Stoffer 2006) was used to identify relationships between NARR meteorological variables, lapse rates, and glacier surface temperatures. Before correlation coefficients (r) were calculated, a centered three-day moving average low-pass filter was applied to all time series. This removed local noise that was present at daily frequencies and improved comparisons between time series from field sites that are separated by up to 700 km and may be affected by the same synoptic events
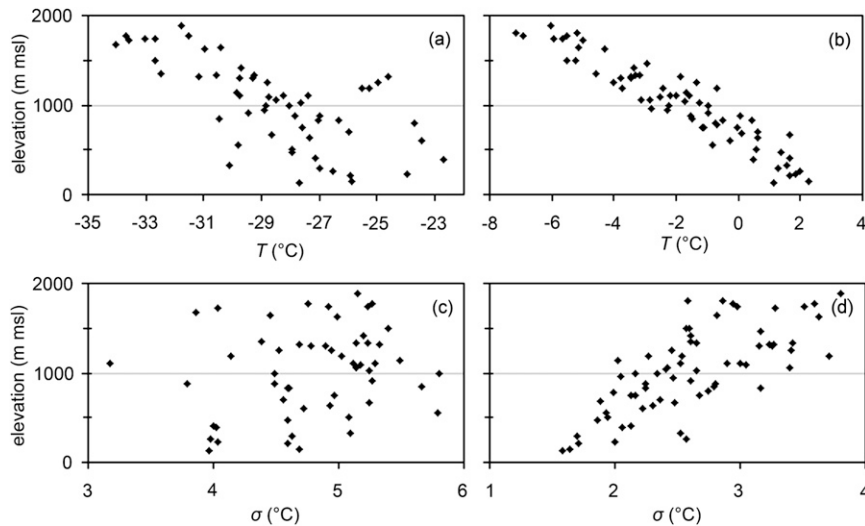
FIG. 3. Average (a) DFJ and (b) JJA near-surface temperatures and (c),(d) their standard deviations with respect to sensor elevation. The relationship between temperature and elevation is much weaker in winter ($r = -0.68$) than in summer ($r = -0.94$) and standard deviations are significantly correlated with elevation in summer ($r = 0.73$) only.

but at different times. As with most subannual meteorological time series, there are strong red noise (seasonal cycle) components in the datasets that must be removed before representative correlation coefficients can be determined. This was accomplished by subtracting monthly means from all time series before correlation coefficients were calculated. The significance of the correlation coefficients was determined using a two-tailed Student's t test with the null hypothesis that the time series were uncorrelated ($r = 0$). The low-pass filter introduces lag-1 and lag-2 serial correlations into the time series that might affect the assessment of the statistical significance of correlation coefficients, although "inferences about the correlation coefficient seem to be relatively weakly affected by serial correlation" (von Storch and Zwiers 1999, p. 149). To err on the side of caution, we adopted a 99% confidence level ($p < 0.01$) as the threshold for statistical significance.

4. Results

a. Near-surface temperatures

Mean annual temperatures averaged over all sensors ranged from $-18.9°$ to $-15.5°C$ for the Agassiz and JEG transects, respectively. Average monthly transect temperatures are lowest in February (from $-35°$ to $-29°C$) and highest in July (from $-1°$ to $+2°C$). There are pronounced seasonal cycles in the monthly mean standard deviations of daily temperatures, with higher standard deviations ($3.5°$ to $7.1°C$) during the winter [December–

February (DJF)] and lower values ($2.0°–3.7°C$) during the summer [June–August (JJA)]. The lower standard deviations in summer are in part due to fixed temperatures ($0°C$) at the melting surface.

The relationship between elevation and seasonal mean temperature is much stronger during the summer (average $r = -0.94$; Fig. 3b) than in the winter (average $r = -0.68$; Fig. 3a). This suggests that a constant regional near-surface lapse rate is a better description of the near-surface temperature field during the summer than in the winter. There is also a significant correlation ($r = 0.73$) between elevation and the standard deviation of the daily near-surface temperatures in summer (Fig. 3d) but not in winter (Fig. 3c). The atmospheric controls governing this observed relationship will be discussed in section 5.

b. Lapse rates

Daily near-surface lapse rates ranged between $-11.9°C$ km^{-1} (recorded during a strong temperature inversion over the JEG transect in March 2003) and $14.8°C$ km^{-1} (recorded over the Devon_S transect in November 2002). Centered 3-day moving average lapse rates for each of the six transects are presented in Fig. 4. Lapse rates are generally lower during colder months and higher during warmer months. Monthly mean values (Fig. 5) are on average $1.8°C$ km^{-1} higher in summer than in winter. Monthly mean daily temperature–elevation correlation coefficients are also larger in summer ($r = 0.82–0.97$) than in winter ($r = 0.63–0.85$),
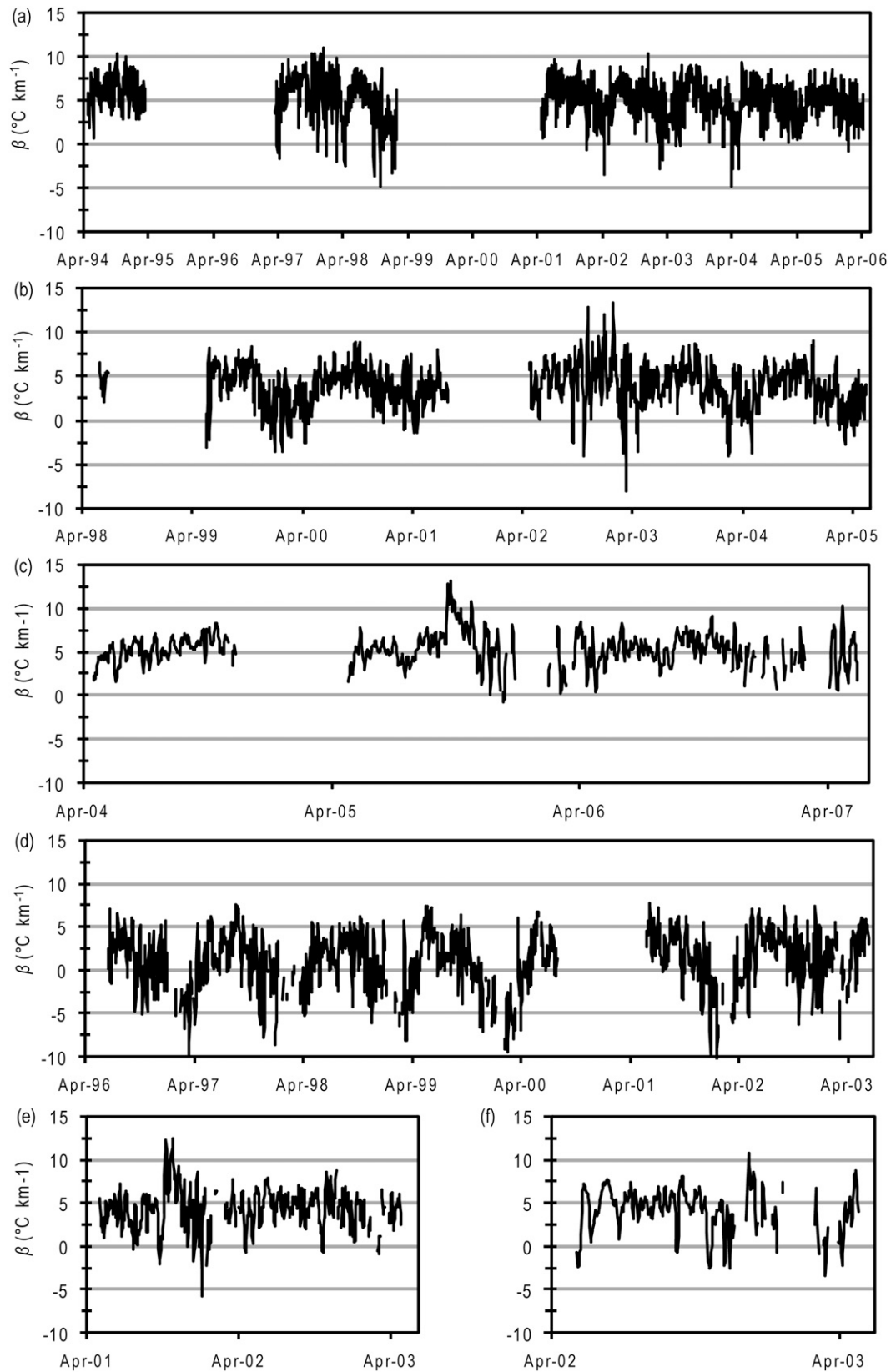
FIG. 4. Three-day moving average lapse rates (β) for the (a) Agassiz, (b) Devon_N, (c) Devon_S, (d) JEG, (e) POW_N, and (f) POW_S transects.
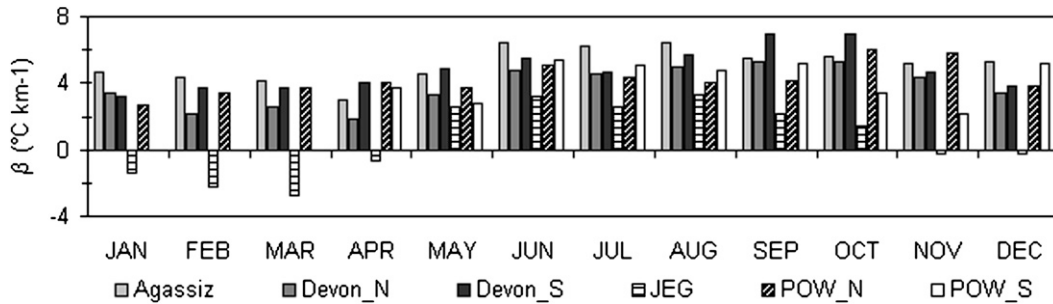
FIG. 5. Monthly mean lapse rates (β) for all six transects.

suggesting that the assumption of a linear near-surface lapse rate is most appropriate during the summer months. Lower lapse rates are expected during winter months because of a persistent lower-troposphere temperature inversion that is observed throughout the Arctic (Serreze and Barry 2005, 139–143). During polar night, when there is little or no solar radiation, an atmospheric temperature inversion results from longwave radiative equilibrium between the highly emissive colder snow surface and the less emissive and warmer lower troposphere. It is maintained by the northward advection of warmer subarctic air (Overland and Guest 1991). The strength of the lower-troposphere temperature inversion is strongly influenced by the presence of diamond dust (Overland and Guest 1991) and occurrence of cloud cover (Serreze et al. 1992). Near-surface lapse rates over JEG are on average 2.2°C km^{-1} lower than lapse rates over the other five transects in summer and 4.4°C km^{-1} lower in winter (Fig. 5). The Agassiz transect has the highest average summer (6.4°C km^{-1}) and winter (4.6°C km^{-1}) lapse rates. This is likely due to the Agassiz transect's generally colder climate, which results in less frequent summer melt and a less extensive melting zone than is observed at the other three sites

(Wang et al. 2005). Less melt area leads to less area at lower elevations with surface temperatures fixed at 0°C, resulting in slightly higher near-surface lapse rate. Lower temperatures also result in higher MALRs because the MALR tends toward the dry air lapse rate as temperatures cool. All other mean summer and winter lapse rates lay within the ranges 4.9° ± 0.4°C km^{-1} and 3.2° ± 0.5°C km^{-1}, respectively. These values are systematically lower than standard MALRs, which is consistent with most previously published values for Arctic glaciers and the Greenland Ice Sheet (Table 1).

Cross correlations between daily lapse rates along the different glacier transects are stronger during summer months than in winter (Table 2). This suggests that regional-scale processes account for a larger fraction of the variance in lapse rates during summer than winter. To illustrate the strength of this regional influence, all available lapse rates for summer 2002 are plotted in Fig. 6.

c. Relationship between near-surface lapse rates and atmospheric conditions

Summer daily mean lapse rates measured over all six temperature–elevation transects are significantly lower

TABLE 1. Previously reported Arctic glacier and ice sheet near-surface temperature lapse rates (β).

Location	Study	Months	β (°C km^{-1})
Devon Island Ice Cap, Nunavut, Canada	Shepherd et al. (2007)	Not given	4.6
Devon Island Ice Cap, Nunavut, Canada	Mair et al. (2005)	JJA	4.8
Greenland Ice Sheet	Steffen and Box (2001)	Annual	7.1
Greenland Ice Sheet	Steffen and Box (2001)	June	4.0
Greenland Ice Sheet	Box and Rinke (2003)	June, July	5.0
Greenland Ice Sheet (>1000 m MSL)	Hanna et al. (2005)	JJA	7.9
Greenland Ice Sheet (≤1000 m MSL)	Hanna et al. (2005)	JJA	4.3
Nigardsbreen, Norway	Jóhannesson et al. (1995)*	Summer	5.8
Ny-Alesund, Spitsbergen	Wright et al. (2005)	Not given	4.0
Prince of Wales Ice Field, Nunavut, Canada	Marshall et al. (2007)	JJA	4.7
Qamanarssup, West Greenland	Jóhannesson et al. (1995)*	Summer	6.6
Storstrommen, Northeast Greenland	Bøggild et al. (1994)	June, August	4.0
Satujokull, Iceland	Jóhannesson et al. (1995)*	Summer	5.3

* Determined through model calibration (not measured).

TABLE 2. Summer (JJA) and winter (DJF) cross correlations between each of the lapse rate time series of the six sensor transects. Significant ($p \le 0.01$) correlations are shown in bold.

	Winter					Summer				
	Agassiz	Devon_N	Devon_S	JEG	POW_N	Agassiz	Devon_N	Devon_S	JEG	POW_N
Devon_N	**0.34**					**0.29**				
Devon_S	**0.25**	—				**0.37**	**0.81**			
JEG	**0.35**	**0.40**	—			**0.45**	**0.25**	—		
POW_N	**0.37**	**0.31**	—	**0.50**		**0.25**	**0.47**	—	**0.83**	
POW_S	—	—	—	—	—	0.09	**0.52**	—	**0.76**	**0.89**

than the free-air MALR when summit elevation temperatures are anomalously high (Fig. 7). The relationship between measured lapse rates and temperatures is strongest when lapse rates are compared with temperature measurements taken at higher elevations. In addition, when near-surface lapse rates are correlated with NARR 500Z and 750T (averaged over each of the four glaciers) the strongest relationships are between summer lapse rates and 750T (Fig. 8).

Variations in summer 750T over the Canadian high Arctic are associated with synoptic-scale southerly advection of warm North American continental air and northerly advection of cold polar air masses that affect temperatures on a regional scale (Alt 1987; Gardner and Sharp 2007). Mean summer correlation coefficients with summer 750T are negative and significant for all lapse rate series and range between $r = -0.55$ and -0.81. These findings show that lower lapse rates are associated with warmer air masses and higher rates with colder air masses.

5. Influence of free-atmospheric temperatures on near-surface temperatures and lapse rates

To explain what drives the relationship between free-air temperatures and near-surface lapse rates we focus on a vertical cross section of the atmospheric boundary layer between the glacier surface and the free atmosphere, and discuss the "climate sensitivity" of the near-surface air temperature. This is defined here as the change in near-surface temperature relative to a change in the free-atmospheric temperature. During the summer, the glacier surface gains energy through a positive net radiation flux and, to a lesser extent, through turbulent heat transfer and rainfall. The snow and glacier ice warm until the surface reaches the melting point, after which further net inputs of energy produce melt while the surface temperature remains fixed at 0°C. Because surface temperatures are fixed over a melting glacier surface and free-atmosphere temperatures decrease with increasing elevation, the free atmosphere becomes warmer relative to the surface as the surface elevation decreases. This gradient drives a flux of sensible heat from the atmosphere to the glacier surface that modifies the temperature of the air within the boundary layer. A larger sensible heat flux will result in greater cooling of the boundary layer relative to the temperature of the free atmosphere, so the climate sensitivity of the near-surface air temperature over a melting surface will be less than unity.

The upper portions of Arctic glaciers will often remain frozen while melt occurs at lower elevations. Where the surface is frozen, the temperature of the snow/ice surface can vary with changes in the free-air temperature. Because of this, vertical temperature gradients in the boundary layer over frozen surfaces are generally not as large as those found over melting surfaces. Thus, near-surface air temperatures over frozen surfaces have larger climate sensitivities than temperatures over melting surfaces. Consistent with this argument, Denby et al.
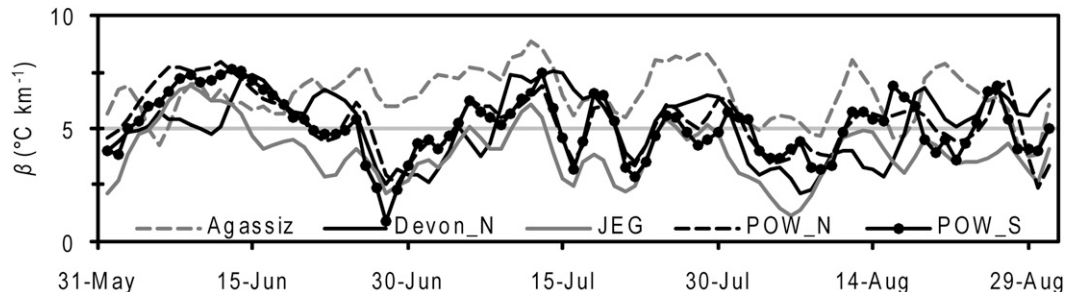

FIG. 6. All available 2002 summer lapse rates (β).
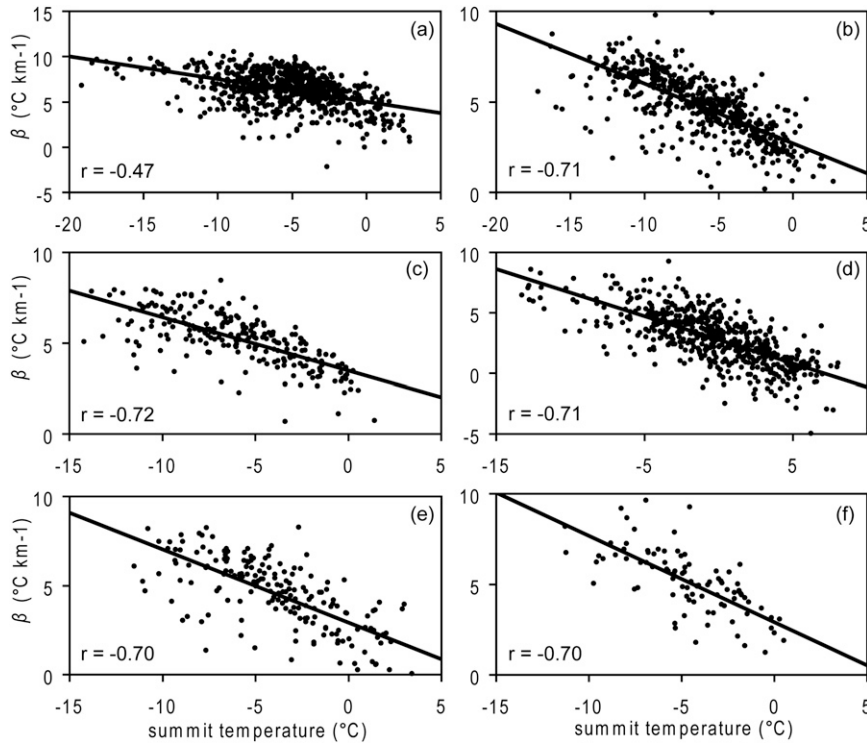
FIG. 7. Summer daily mean lapse rates (β) plotted against measured summit elevation temperatures for the (a) Agassiz, (b) Devon_N, (c) Devon_S, (d) JEG, (e) POW_N, and (f) POW_S temperature–elevation transects with heavy black lines showing the linear regression relationship between the two variables.

(2002) showed that the climate sensitivity of near-surface air temperatures over the Greenland Ice Sheet was close to unity in the dry snow zone (no melt) and that it decreased with elevation to a value of only 0.3 in the lower ablation zone. This explains the observed increase in the standard deviation of glacier near-surface temperatures at higher surface elevations (Fig. 3d).

The sensible heat flux, and therefore the degree to which the temperature of the atmospheric boundary layer air is modified, is also influenced by the wind speed.

Observations (van den Broeke 1997) and modeling studies (Denby et al. 2002) in Greenland show that downslope glacier winds increase systematically with increases in free-atmospheric temperatures during the ablation season. This has the effect of increasing the sensible heat flux at lower elevations when warm air is advected into the region. However, the climate sensitivity of the glacier wind is relatively low (0–0.2 m s^{-1} °C^{-1}), so changes in the near-surface temperature will be primarily governed by changes in the sensible heat flux that
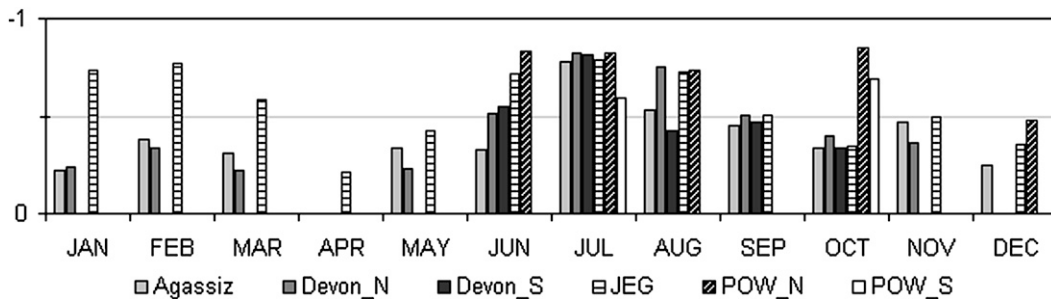

FIG. 8. Mean monthly correlation coefficients between lapse rates and 750T. Only those values significant at the 0.01 level are shown.

result from changes in free-air temperatures (Denby et al. 2002). Glacier winds over the ice masses examined in this study are not as well developed as those observed over the Greenland Ice Sheet and will have less impact on the sensible heat flux variability than was observed by Denby et al. (2002). Summer mean daily wind speed and direction measurements from three weather stations located on JEG and three stations located on the Devon Island Ice Cap show an increase in the frequency of downslope (katabatic) winds at lower elevations, but neither transect shows an increase in mean wind speed at lower elevations or any consistent relationship between wind speed and 750T.

The relationship between the climate sensitivity of near-surface temperature and elevation means that, when warm air is advected into the region, near-surface temperatures over glaciers will not rise uniformly. Because of larger near-surface air temperature sensitivities at higher elevations, near-surface air temperature will increase more at higher elevations than at lower elevations in response to an increase in free-atmospheric temperature. This has the effect of reducing the lapse rate, consistent with the strong negative correlation between 750T and lapse rates (Fig. 8). Ablation season dependence of surface roughness on elevation (preference for snow at higher elevations and ice at lower elevations) may also play a role in modifying the glacier near-surface lapse rate but is not investigated in this study.

6. Implications for the modeling of near-surface temperatures

During the melt season, the variability in measured lapse rates is strongly related to the variability in 750T (Fig. 8). This relationship was used to develop simple empirical models to predict daily near-surface lapse rates from standardized daily anomalies in 750T (summer means removed and divided through by respective standard deviation). Using least squares regression analysis, model coefficients were calculated for each of the four glaciers (Table 3). Because the regression models are based on standardized anomalies (mean = 0), all model y intercepts (β) are equal to respective glacier mean summer lapse rates. Where more than one daily lapse rate measurement was available for the same glacier (i.e., Devon and POW), the lapse rate was taken to be the mean of the two estimated values.

Nonablation season lapse rates are important for the determination of end-of-winter snowpack temperatures. However, the relationship between free-air temperatures and lapse rates breaks down outside the ablation season and there is no strong relationship between nonablation season lapse rates and either winds or

TABLE 3. Best-fit linear regression slope (m), mean summer (β, y intercept), and nonablation season (β_w) lapse rates and r values for modeling summer near-surface lapse rates with 750T standardized anomalies.

	Agassiz	Devon	JEG	POW
m ($\degree$C km^{-1})	−0.83	−0.84	−1.31	−1.39
β ($\degree$C km^{-1})	6.4	4.9	3.1	4.6
β_w ($\degree$C km^{-1})	4.8	4.0	0.4	4.2
r		0.55	0.61	0.75	0.80

geopotential height that can be used to model them. Thus we chose not to attempt to downscale winter temperatures. If winter temperatures are needed for a mass balance modeling study, we suggest setting the lapse rate for days outside the ablation season to the mean nonablation season lapse rate (Table 3). A lapse rate minimum threshold of $0\degree$C km^{-1} should also be applied to summer values to prevent unrealistically low lapse rates during extreme warm periods. This threshold does not impact the results presented here but might be relevant if the lapse rate models developed here were applied to years that are anomalously warm compared to the years examined in this study.

a. Validation of temperature extrapolation methods

Prior to comparing long-term differences in surface air temperature estimates made using modeled daily lapse rates with those made using a constant MALR ($6.5\degree$C km^{-1}), the modeled daily lapse rate downscaling method was validated over the Devon Island Ice Cap for the summer of 2006. Coefficients for the Devon lapse rate model were first calibrated by excluding 2006 data. Daily lapse rates were then calculated for the 2006 melt season using daily NARR 750T standardized anomalies. Daily observed, modeled, and constant measured mean summer ($5.1\degree$C km^{-1}) lapse rates are plotted together with the MALR ($6.5\degree$C km^{-1}) in Fig. 9. There is reasonably good consistency between the patterns of variability in the observed and modeled lapse rates ($r = 0.68$) and their means, which are not statistically different when compared using a two-tailed Student's t test with the null hypothesis that the means are equal. Both lapse rates are significantly lower than the MALR.

For the validation process, least squares linear regression was used to reconstruct daily summit elevation temperatures (1880 m) by extrapolating 2006 daily temperature measurements made along the Devon_S transect. This effectively minimizes the local error associated with single-station measurements and provides a temporally continuous summit elevation temperature that can be extrapolated to lower elevations using a specified lapse rate.
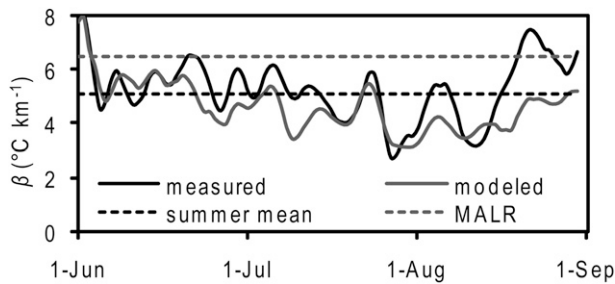
FIG. 9. Three-day average measured and modeled near-surface lapse rates (β) for Devon Island Ice Cap. The mean measured summer lapse rate (5.1°C km^{-1}) and the MALR (6.5°C km^{-1}) are plotted for comparison. Modeled lapse rates were calculated using 750T anomalies and linear regression coefficients calibrated with temperature–elevation data from previous years. Measured and modeled lapse rates are fully independent and are significantly correlated ($r = 0.68$).

To assess the errors associated with lapse rate choice when downscaling near-surface temperatures, measured and modeled daily lapse rates, a constant lapse rate equal to the 2006 summer mean (5.1°C km^{-1}), and the MALR were used to extrapolate reconstructed summit temperatures to the elevation of each Devon_S transect temperature sensor with a complete 2006 summer record. Taking the daily mean temperature measured at each station as the true temperature, mean and standard errors in daily mean temperatures were determined for each of the four extrapolation methods (Fig. 10). Averaged over all stations, temperatures extrapolated using mean daily and summer measured lapse rates have

a mean error of zero as they have been derived directly from the 2006 summer station data (Fig. 10a). Temperatures extrapolated using modeled lapse rates have a small mean cold bias (-0.3°C) while those extrapolated using the MALR have a strong warm bias (0.8°C) that decreases with increasing elevation. Compared with air temperatures extrapolated using a constant lapse rate, modeled daily lapse rates offer a slight improvement in the standard error of the estimated temperatures (Fig. 10b).

A similar error analysis for estimates of positive degree-days (PDDs), a quantity that is strongly related to glacier melt (Braithwaite 1981; Hock 2003), reveals that only those extrapolation methods that employ variable lapse rates can reproduce the observed annual PDD values (mean error $\approx 0° \pm 10$°C day yr^{-1}; Figs. 10c,d). Because near-surface lapse rates vary systematically with temperature, employing the constant mean summer lapse rate results in temperature underestimation during relatively cold periods and overestimation during relatively warm periods. Across all stations, this results in an average PDD overestimation of 25°C day yr^{-1}, with a mean error as high as 75°C day yr^{-1} at the lowest station. Using the MALR greatly overestimates total PDDs with mean errors as high as 160°C day yr^{-1}.

b. Comparison between PDDs downscaled using daily modeled lapse rates and a constant MALR

To illustrate differences in surface air temperature estimates when differing lapse rates are employed, we
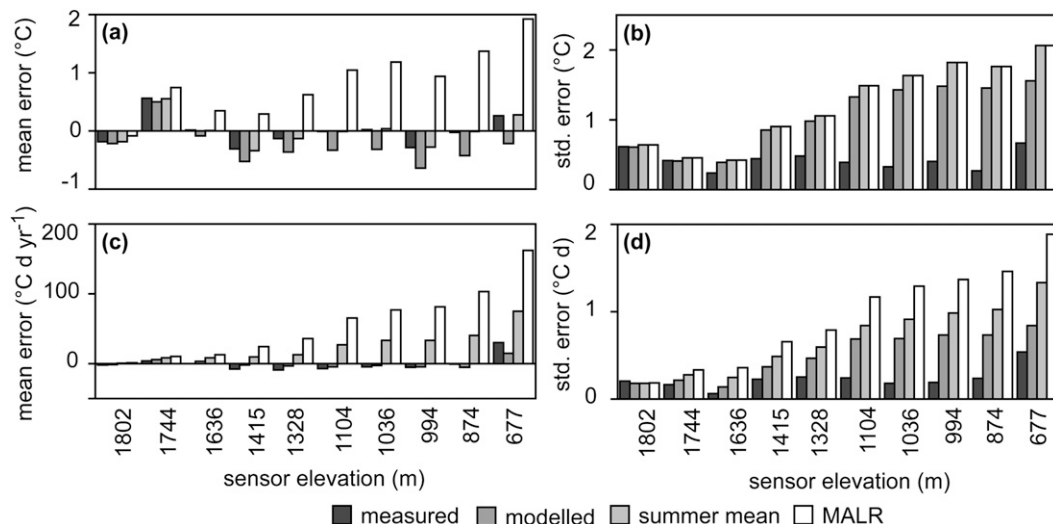

FIG. 10. (left) Mean and (right) standard error in (a),(b) near-surface temperatures and (c),(d) positive degree-days extrapolated from reconstructed summit elevation temperatures using variable daily mean measured and modeled lapse rates as well as constant lapse rates equal to the 2006 mean summer lapse rate (5.1°C km^{-1}) and MALR (6.5°C km^{-1}).
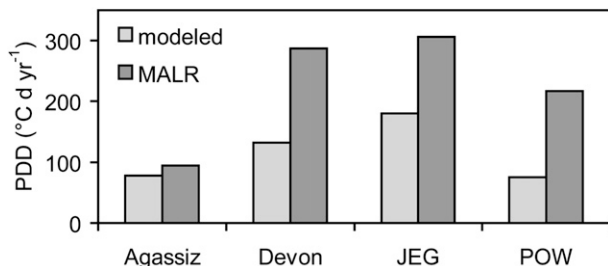
FIG. 11. The 1994–2006 area averaged mean annual PDDs for the Agassiz Ice Cap, Devon Island Ice Caps, JEG, and POW derived from near-surface temperature fields downscaled from NARR 750T using daily modeled and a constant lapse rate set equal to the MALR ($6.5°C$ km^{-1}).

compared daily mean temperatures downscaled to glacier surfaces [Canada3D digital elevation model (DEM), available from Natural Resources Canada] from NARR 750T using both daily modeled lapse rates and the MALR for the period 1994–2006. Results are displayed as total PDDs. As part of the downscaling process, 750T was first adjusted to the temperature at the highest available station on each glacier by subtracting the monthly mean difference between 750T and the station temperatures. The derived station temperature was then downscaled over the entire glacier surface at the 3D DEM resolution (30 s approximately 900×200 m) using the two different lapse rates.

Using the model coefficients provided in Table 3 and daily 750T standardized anomalies, mean annual total PDDs for the period 1994–2006 were estimated for each of the four glaciers (Fig. 11). Average annual PDD totals for the Agassiz Ice Cap, Devon Island Ice Cap, John Evans Glacier, and Prince of Wales Ice Field were 80°, 130°, 180°, and $80°C$ day yr^{-1}, respectively. Averaged over each glacier, the annual total PDDs derived from near-surface temperatures downscaled using daily mod-

eled lapse rates are 20°, 160°, 130°, and $140°C$ day yr^{-1} less than PDD totals generated using the constant MALR for the Agassiz and Devon Island Ice Caps, John Evans Glacier, and Prince of Wales Ice Field, respectively. Except for the Agassiz Ice Cap (which has the lowest mean summer temperatures, one of the lowest estimated average annual PDD totals, and the highest near-surface temperature lapse rates), downscaling with the MALR results in a substantial overestimation of near-surface air temperatures and annual PDDs. In the case of the Prince of Wales Ice Field, using the MALR produces annual PDD estimates nearly 3 times those derived using modeled lapse rates. This large difference is due not only to the nearly $2°C$ km^{-1} difference between the mean of the modeled lapse rate and the MALR but also to (i) the large vertical distance over which temperatures are downscaled (~1800 m), (ii) the high sensitivity of lapse rates to changes in 750T standardized anomalies ($-1.39°C$ km^{-1}), (iii) low annual PDD totals, and (iv) the large number of days (averaged over all stations: 43 days yr^{-1}) with near-surface temperatures within $\pm2°C$ of the freezing point.

To illustrate the spatial differences in PDD estimates, mean annual PDDs estimated from surface air temperatures downscaled using modeled daily lapse rates (Fig. 12a) and the MALR (Fig. 12b) are shown for the Devon Island Ice Cap. Because both downscaling methods extrapolate from the same summit point location temperature series, our model comparisons show good agreement between downscaling methods near summit elevations and larger disagreement at lower elevations. If adjusted sea level temperatures had been extrapolated instead, the MALR would result in an underestimate of near-surface temperatures and total PDDs relative to those determined using modeled daily lapse rates, as opposed to the overestimates reported here.
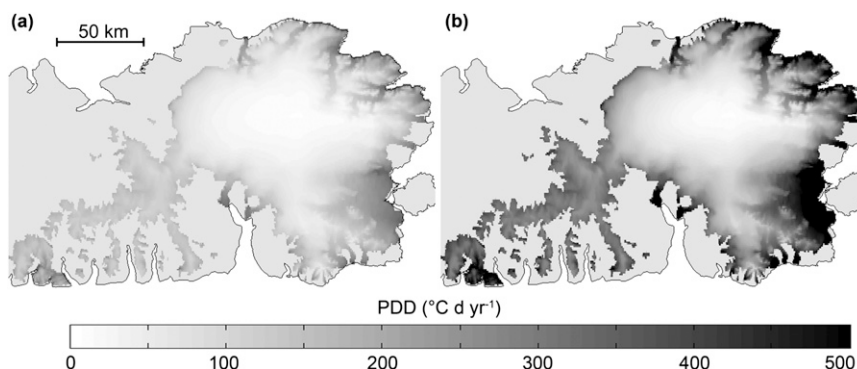

FIG. 12. The 1994–2006 mean annual PDDs for the Devon Island Ice Caps derived from near-surface temperature fields downscaled from NARR 750T using (a) daily modeled lapse rates and (b) a constant lapse rate equal to the MALR.

7. Discussion

Consistent with previous studies (Greuell and Böhm 1998; Steffen and Box 2001; Lowe and Porter 2004; Hanna et al. 2005; Mair et al. 2005; Wright et al. 2005; Marshall et al. 2007; Shepherd et al. 2007), we found that ablation season near-surface lapse rates observed over Arctic glacier surfaces are consistently lower than the MALR. Higher near-surface lapse rates of $7°$–$9°C\,km^{-1}$ have been reported for some valley glaciers (Schuler et al. 2005; Brock et al. 2006). In these cases, however, lapse rates were derived using air temperatures measured at two weather stations, one of which was located at a higher elevation on glacier ice and the other at a lower elevation on exposed ice-free ground. This has the effect of producing artificially high near-surface glacier lapse rates because the temperatures recorded at the lower weather stations are not as strongly affected by the cooling effects of the glacier surface as those at the upper stations. Using these lapse rates to extrapolate near-surface temperatures over large altitudinal distances over ice could result in significant errors.

Near-surface lapse rates over glaciers vary on seasonal and daily time scales, a phenomenon that, although well documented (Braun and Hock 2004; Steffen et al. 2004; Hanna et al. 2005; Marshall et al. 2007), is rarely accounted for in the downscaling or extrapolation of near-surface air temperatures (Greuell and Böhm 1998; Gardner and Sharp 2009). Unlike previous studies, our work has shown that the variability in glacier near-surface lapse rates during summer months is significantly correlated on a regional scale and that this covariability appears to be controlled by regional-scale changes in lower-troposphere (750 mbar) temperatures that are associated with the passage of synoptic weather systems (Alt 1987; Gardner and Sharp 2007; Marshall et al. 2007). During the ablation season, the sensitivity of glacier near-surface air temperature to changes in free-atmosphere temperature increases with elevation (Denby et al. 2002). This is because surface temperatures are fixed at $0°C$ over melting glacier surfaces, while free-atmosphere temperatures decrease with increasing elevation. As the surface elevation decreases, the free atmosphere becomes warmer relative to the surface, which drives a sensible heat flux that cools the atmospheric boundary layer at a rate that is proportional to the vertical temperature gradient. The less frequent occurrence of melt at higher elevations reinforces this relationship, as near-surface temperatures have a higher climate sensitivity over frozen surfaces than over melting surfaces (Denby et al. 2002). To a lesser extent, glacier winds (which are known to increase in strength with the magnitude of the atmospheric boundary layer temperature inversion; van den Broeke 1997) also support

an increase in sensible heat flux with decreasing elevation (Denby et al. 2002). Therefore, near-surface air temperatures will increase more at higher elevations than at lower elevations in response to an increase in free-atmospheric temperature. This effectively reduces the near-surface lapse rate and results in the negative relationship between 750T and near-surface lapse rates.

This relationship was used successfully to develop glacier-specific models for the downscaling of coarse-resolution temperature fields. Through the model validation process it was shown that summer near-surface air temperatures downscaled using modeled daily lapse rates substantially improve estimates of total PDDs over glaciers relative to use of a constant lapse rate equal to either the mean ablation season lapse rate or the MALR. When lower-troposphere temperatures were downscaled over each of the four glaciers examined in this study for the period from 1994 to 2006, the use of a constant MALR overestimated annual total PDDs by an average of $110 \pm 64°C\,day\,yr^{-1}$ relative to values estimated using modeled lapse rates. In the case of the Prince of Wales Ice Field, annual mean PDDs estimated using a constant MALR were nearly 3 times greater than those estimated using modeled lapse rates. The chronic overestimation of PDDs when the MALR is employed can result in significant errors in glacier mass balance estimates when the near-surface temperature is used to model glacier melt. Following a similar methodology to the one outlined here, Gardner and Sharp (2009) showed that, for the Devon Island Ice Cap over the period 1980–2006, estimates of glacier mass balance made using a degree-day model can be as much as 4 times more negative when summit elevation temperatures are downscaled with the MALR than estimates made using a variable lapse rate modeled from lower-troposphere temperatures and 2.5 times more negative when downscaling is performed using a mean measured summer lapse rate.

Despite good regional correlations and success at downscaling temperatures over individual glaciers, lapse rate model coefficients differ between glaciers (Table 3). There is generally good agreement in the model slopes (m) (from -0.83 to $-1.39°C\,km^{-1}$), but mean summer lapse rates (β : y intercept) vary greatly ($6.4°$–$3.1°C\,km^{-1}$) between glaciers. This suggests that lapse rate models should be calibrated for individual glaciers. If it is necessary to downscale temperatures over Arctic glaciers for which there are insufficient measurements to calibrate a model, we suggest using $m = -1.1°C\,km^{-1}$ and $\beta = 4.9°C\,km^{-1}$. These model parameters correspond to the average model slope for the four glacier-specific models (Table 3) and the mean ablation season lapse rate for the six transects and all previously published Arctic ablation season lapse rates included in Table 1.

For the four glaciers examined in this study, applying this model to downscale 750T to near-surface temperatures for the period of 1994–2006 produces total PDD estimates that are on average $17° \pm35°C$ day yr^{-1} larger than total PDD estimates derived using the site-specific lapse rate models. Similar estimates made using a constant lapse rate equal to the mean ablation season lapse rate $(4.9°C\,km^{-1})$ produce total PDD estimates that are on average $33° \pm46°C$ day yr^{-1} too large.

In this study, near-surface lapse rates were parameterized using standardized 750-mbar temperature anomalies because temperatures at this pressure level are representative of free-air temperatures for all four glaciers examined and provide the highest correlations (not shown) with near-surface lapse rates when compared to surface and other lower- and midtroposphere temperatures. This being said, model coefficients are relatively insensitive to the temperature used for the parameterization of the lapse rate model. Parameterizations based on NARR surface, 900-, 850-, or 500-mbar standardized temperature anomalies, derived in the same way as for 750T, result in model slopes that are within $\sim\pm20\%$ of those reported for the glacier-specific lapse rate models based on 750T (Table 3) and within $\sim\pm15\%$ of the regional model. All alternative models have the same mean lapse rate (intercept) but have slightly lower regression coefficients when averaged across all four glaciers. Standardized surface air temperature anomalies provide the poorest model fit, as they are the least representative of free-air temperatures.

Near-surface air temperatures were downscaled from glacier summit temperatures to lower elevations. This approach was used because NARR temperatures (surface or lower-troposphere) show increased correlation with on-glacier temperature measurements as the elevation of the on-glacier measurement increases. This suggests that NARR, and likely other regional/global climate models, does a better job at simulating higher-elevation temperatures (which are closer to free-air values) than temperatures at lower elevations [which are more strongly influenced by complex local effects, e.g., topography, katabatic winds, higher frequency of surface melt (stronger sensible heat flux), and increased influence from low-lying cloud]. Our approach to downscaling involves two steps: interpolating the NARR lower-troposphere temperatures to an elevation on the ice cap and then downscaling from that elevation using a computed lapse rate. Errors arising from the first step are minimized by interpolating measured temperatures to the ice cap summit elevation, while those arising from the lapse-rate-based downscaling are independent of the choice of height from which to interpolate. Thus total error in surface air temperature estimates should be minimized by the approach that we have adopted.

8. Conclusions

The negative relationship between near-surface lapse rates and lower-troposphere temperatures suggests that lower lapse rates can be expected under a warming climate. This trend is driven by the increase in free-air temperatures, the migration of the glacier melt zone to higher elevations earlier in the season (larger glacier area with a fixed surface temperature) and, to a lesser extent, by enhanced glacier winds. This means that, as ablation season temperatures warm over the Arctic, temperatures near the glacier surface may become less sensitive to temperature changes in the free atmosphere. If this behavior were incorporated into glacier mass balance models, it could reduce projections of Arctic glacier melt and its contributions to sea level in a warmer climate. The opposite would be true if variable lapse rates were used to extrapolate terminus (lower elevation) near-surface temperatures to higher elevations.

APPENDIX

Temperature Sensors Used in Study

Transect temperature sensor details (Table A1) and sensor accuracies (Table A2) are provided in the following tables. All quality controlled daily average

TABLE A1. Temperature sensor identification (ID), sensor type, location, and periods of operation.

Transect ID	Station ID	Sensor type	Lat (°N)	Lon (°W)	Elevation (m MSL)	First month of record	Last month of record
Agassiz	A_1	107F	80.80	72.90	1736	Jun 1988	Apr 2006
	A_2	107F	80.83	71.90	1314	Jun 1991	Apr 2006
	A_3	107F	80.87	71.28	878	Apr 1994	Apr 2006
Devon_N	D1_N	107F	75.34	82.10	1880	Apr 1997	May 2005
	D2_N	107F	75.37	82.67	1780	Mar 1992	Mar 1995
	D3_N	107F	75.39	82.76	1768	Apr 2000	May 2005
	D4_N	107F	75.42	82.95	1628	May 1999	Aug 2003
	D5_N	107F	75.49	83.28	1339	May 1998	May 2005
	D6_N	107F	75.69	83.26	330	Apr 1997	May 2005
Devon_S	D1_S	107F	75.34	82.68	1802	May 2005	Jan 2007
	D2_S	107F	75.18	82.78	1415	Jun 2004	May 2007
	D3_S	107F	75.01	82.88	994	May 2005	May 2007
	Km0	HOBO	75.34	82.68	1802	May 2004	Sep 2004
	Km4.7	HOBO	75.30	82.70	1744	Apr 2004	May 2007
	Km8	HOBO	75.27	82.72	1676	Sep 2004	Feb 2005
	Km9.1	HOBO	75.26	82.73	1636	Apr 2004	Mar 2007
	Km13.6	HOBO	75.22	82.75	1502	Apr 2004	Dec 2006
	Km21.4	HOBO	75.15	82.79	1328	Apr 2004	May 2007
	Km24.6	HOBO	75.12	82.81	1255	Apr 2004	May 2007
	km27.9	HOBO	75.09	82.83	1194	Apr 2004	Aug 2004
	km30.2	HOBO	75.07	82.84	1146	May 2005	Apr 2006
	km31.4	HOBO	75.06	82.85	1104	Apr 2006	Feb 2007
	Km34.6	HOBO	75.03	82.86	1036	Apr 2006	Dec 2006
	Km36.8	HOBO	75.01	82.88	994	Apr 2004	Feb 2007
	Km39.2	HOBO	74.99	82.89	966	Apr 2004	Aug 2004
	Km41.7	HOBO	74.97	82.90	874	Apr 2004	Feb 2007
	Km43.7	HOBO	74.95	82.92	786	Apr 2004	Sep 2005
	km45.7	HOBO	74.94	82.93	677	Apr 2004	Dec 2006
	Km47.7	HOBO	74.92	82.94	478	Apr 2004	Nov 2006
JEG	UWS	35CF	79.71	74.56	1183	Jun 1996	Jul 2002
	MWS	35CF	79.67	74.35	824	Jun 1996	Jul 2002
	LWS	35CF	79.63	74.08	261	Jun 1996	Jul 2002
	1500m	HOBO	79.72	74.50	1470	May 2001	Jun 2003
	1300m-W	HOBO	79.70	74.55	1320	Jun 2002	May 2003
	1300m-E	HOBO	79.71	74.49	1324	May 2001	Jun 2003
	1250m	HOBO	79.72	74.55	1245	May 2001	Jun 2002
	1200m	HOBO	79.71	74.56	1185	May 2002	Jun 2003
	1100m	HOBO	79.70	74.53	1110	May 2001	Jun 2003
	1000m	HOBO	79.69	74.50	1026	May 2001	Jun 2003
	900m	HOBO	79.68	74.44	915	May 2001	Jun 2003
	800m	HOBO	79.67	74.35	825	May 2002	May 2003
	700m	HOBO	79.67	74.30	705	May 2001	Jun 2003
	600m	HOBO	79.65	74.30	630	May 2001	May 2003
	500m	HOBO	79.64	74.19	510	May 2001	May 2003
	400m	HOBO	79.65	74.11	400	May 2001	Jun 2003
	300m	HOBO	79.64	74.08	300	May 2001	Jun 2003
	250m	HOBO	79.63	74.08	235	Jun 2002	May 2003
	200m	HOBO	79.63	74.08	209	May 2001	May 2003
	140m	HOBO	79.62	74.07	140	Jun 2001	May 2003
POW_N	P_AWS	107	78.49	79.43	1727	Jun 2001	Sep 2002
	WL1300	HOBO	78.50	80.23	1300	May 2001	May 2003
	WL1100	HOBO	78.64	81.20	1094	May 2001	May 2003
	SL1060	HOBO	78.60	79.86	1060	May 2001	Jun 2002
	SL850	HOBO	78.64	79.53	850	May 2001	May 2003
	WL750	HOBO	78.71	81.23	747	May 2001	May 2003

TABLE A1. (*Continued*)

Transect ID	Station ID	Sensor type	Lat (°N)	Lon (°W)	Elevation (m MSL)	First month of record	Last month of record
	WL610	SP-2000	78.68	79.10	660	Apr 2002	May 2003
	LL1500	HOBO	78.55	79.07	1500	Apr 2002	May 2003
	LL1300	HOBO	78.61	78.67	1308	May 2001	May 2003
	LL1100	HOBO	78.63	78.47	1105	May 2001	May 2003
	LL800	HOBO	78.71	76.36	799	May 2001	Apr 2002
	LL600	HOBO	78.72	75.98	602	May 2001	May 2003
	LL400	HOBO	78.70	75.47	395	May 2001	May 2003
	LL130	HOBO	78.68	74.97	129	May 2001	Jan 2003
POW_S	P_STH	SP-2000	77.87	80.81	1350	May 2002	May 2003
	HM1050	HOBO	78.03	81.25	1056	May 2002	May 2003
	HM740	HOBO	78.05	81.65	740	May 2002	Oct 2002
	KR960	HOBO	77.71	80.25	945	May 2002	May 2003
	KR750	HOBO	77.64	80.00	750	May 2002	Jan 2003
	KR550	SP-2000	77.53	79.54	550	May 2002	May 2003

TABLE A2. Temperature sensor measurement range and accuracy.

Sensor type	Manufacturer	Temperature range	Accuracy (worst case)	Accuracy (at 0°C)
107F	Campbell Scientific Ltd.	−53 to +48°C	±0.5°C	±0.2°C
107	Campbell Scientific Ltd.	−35 to +50°C	±0.9°C	±0.3°C
HMP 35CF	Vaisala	−53 to +48°C	±0.5°C	±0.2°C
HOBO H8-PRO	Onset Scientific Ltd.	−30 to +50°C	±1.0°C	±0.2°C
SP-2000	Veriteq Instruments Inc.	−35 to +85°C	±1.0°C	±0.2°C

temperature measurements for each transect are available as supplementary material online at the University of Alberta Arctic and Alpine Research Group's Web site (http://arctic.eas.ualberta.ca/).

REFERENCES

Alt, B. T., 1987: Developing synoptic analogs for extreme mass balance conditions on Queen Elizabeth Island ice caps. *J. Climate Appl. Meteor.,* **26,** 1605–1623.

Arendt, A., and M. Sharp, 1999: Energy balance measurements on a Canadian High Arctic glacier and their implications for mass balance modelling. *Proc. IUGG Symp., Birmingham 1999: Interactions Between the Cryosphere, Climate and Greenhouse Gases,* Birmingham, United Kingdom, International Union of Geodesy and Geophysics, 165–172.

Arnold, N. S., W. G. Rees, A. J. Hodson, and J. Kohler, 2006: Topographic controls on the surface energy balance of a High Arctic valley glacier. *J. Geophys. Res.,* **111,** F02011, doi:10.1029/2005JF000426.

Bassford, R. P., M. J. Siegert, J. A. Dowdeswell, J. Oerlemans, A. F. Glazovsky, and Y. Y. Macheret, 2006a: Quantifying the mass balance of ice caps on Severnaya Zemlya, Russian High Arctic. I: Climate and mass balance of the Vavilov Ice Cap. *Arct. Antarct. Alp. Res.,* **38,** 1–12.

——, ——, and ——, 2006b: Quantifying the mass balance of ice caps on Severnaya Zemlya, Russian High Arctic. II: Modeling the flow of the Vavilov Ice Cap under the present climate. *Arct. Antarct. Alp. Res.,* **38,** 13–20.

Bøggild, C. E., N. Reeh, and H. Oerter, 1994: Modelling ablation and mass-balance sensitivity to climate change of Storstrommen, northeast Greenland. *Global Planet. Change,* **9,** 79–90.

Boon, S., M. Sharp, and P. Nienow, 2003: Impact of an extreme melt event on the runoff and hydrology of a High Arctic glacier. *Hydrol. Processes,* **17,** 1051–1072.

Bougamont, M., J. L. Bamber, and W. Greuell, 2005: A surface mass balance model for the Greenland Ice Sheet. *J. Geophys. Res.,* **110,** F04018, doi:10.1029/2005JF000348.

Box, J. E., and A. Rinke, 2003: Evaluation of Greenland Ice Sheet surface climate in the HIRHAM regional climate model using automatic weather station data. *J. Climate,* **16,** 1302–1319.

Braithwaite, R. J., 1981: On glacier energy balance, ablation, and air temperature. *J. Glaciol.,* **27,** 381–391.

——, and S. C. B. Raper, 2002: Glaciers and their contribution to sea level change. *Phys. Chem. Earth,* **27,** 1445–1454.

Braun, M., and R. Hock, 2004: Spatially distributed surface energy balance and ablation modelling on the ice cap of King George Island (Antarctica). *Global Planet. Change,* **42,** 45–58.

Brock, B. W., I. C. Willis, and M. J. Sharp, 2006: Measurement and parameterization of aerodynamic roughness length variations at Haut Glacier d'Arolla, Switzerland. *J. Glaciol.,* **52,** 281–297.

Cogley, J. G., W. P. Adams, M. A. Ecclestone, F. Jung-Rothenhäusler, and C. S. L. Ommanney, 1996: Mass balance of White Glacier, Axel Heiberg Island, NWT, Canada, 1960-91. *J. Glaciol.,* **42,** 548–563.

Denby, B., W. Greuell, and J. Oerlemans, 2002: Simulating the Greenland atmospheric boundary layer. Part II: Energy balance and climate sensitivity. *Tellus,* **54A,** 529–541.

de Woul, M., R. Hock, M. Braun, T. Thorsteinsson, T. Johannesson, and S. Halldorsdottir, 2006: Firn layer impact on glacial runoff: A case study at Hofsjoekull, Iceland. *Hydrol. Processes,* **20,** 2171–2185.

Fisher, D. A., R. M. Koerner, and N. Reeh, 1995: Holocene climatic records from Agassiz Ice Cap, Ellesmere Island, NWT, Canada. *Holocene,* **5,** 19–24.

Flowers, G. E., and G. K. C. Clarke, 2002: A multicomponent coupled model of glacier hydrology 2. Application to Trapridge Glacier, Yukon, Canada. *J. Geophys. Res.,* **107,** 2288, doi:10.1029/2001JB001124.

Gardner, A. S., and M. Sharp, 2007: Influence of the Arctic circumpolar vortex on the mass balance of Canadian high Arctic glaciers. *J. Climate,* **20,** 4586–4598.

——, and ——, 2009: Sensitivity of net mass balance estimates to near-surface temperature lapse rates when employing the degree-day method to estimate glacier melt. *Ann. Glaciol.,* **50,** 80–86.

Glickman, T., Ed., 2000: *Glossary of Meteorology.* 2nd ed. Amer. Meteor. Soc., 855 pp.

Glover, R. W., 1999: Influence of spatial resolution and treatment of orography on GCM estimates of the surface mass balance of the Greenland Ice Sheet. *J. Climate,* **12,** 551–563.

Gregory, J. M., and J. Oerlemans, 1998: Simulated future sea-level rise due to glacier melt based on regionally and seasonally resolved temperature changes. *Nature,* **391,** 474–476.

Greuell, W., and R. Böhm, 1998: 2 m temperatures along melting mid-latitude glaciers, and implications for the sensitivity of the mass balance to variations in temperature. *J. Glaciol.,* **44,** 9–20.

Hanna, E., P. Huybrechts, I. Janssens, J. Cappelen, K. Steffen, and A. Stephens, 2005: Runoff and mass balance of the Greenland Ice Sheet: 1958-2003. *J. Geophys. Res.,* **110,** D13108, doi:10.1029/2004JD005641.

Hock, R., 2003: Temperature index melt modelling in mountain areas. *J. Hydrol.,* **282,** 104–115.

Jóhannesson, T., O. Sigurdsson, T. Laumann, and M. Kennett, 1995: Degree-day glacier mass-balance modeling with applications to glaciers in Iceland, Norway and Greenland. *J. Glaciol.,* **41,** 345–358.

Koerner, R. M., 2005: Mass balance of glaciers in the Queen Elizabeth Islands, Nunavut, Canada. *Ann. Glaciol.,* **42,** 417–423.

——, and D. A. Fisher, 1990: A record of Holocene summer climate from a Canadian High-Arctic ice core. *Nature,* **343,** 630–631.

Lowe, A. T., and P. R. Porter, 2004: Variability of air temperatures lapse rates: Preliminary results from the Karakoram Himalaya, Pakistan. *Geophysical Research Abstracts,* Vol. 6, Abstract 04441. [Available online at http://www.cosis.net/abstracts/EGU04/04441/EGU04-J-04441.pdf.]

Mair, D., D. Burgess, and M. Sharp, 2005: Thirty-seven year mass balance of Devon Ice Cap, Nunavut, Canada, determined by shallow ice coring and melt modeling. *J. Geophys. Res.,* **110,** F01011, doi:10.1029/2003JF000099.

Marshall, S. J., H. Bjornsson, G. E. Flowers, and G. K. C. Clarke, 2005: Simulation of Vatnajökull ice cap dynamics. *J. Geophys. Res.,* **110,** F03009, doi:10.1029/2004JF000262.

——, M. J. Sharp, D. O. Burgess, and F. S. Anslow, 2007: Surface temperature lapse rate variability on the Prince of Wales Icefield, Ellesmere Island, Canada: Implications for regional-scale downscaling of temperature. *Int. J. Climatol.,* **27,** 385–398.

Meier, M. F., M. B. Dyurgerov, U. K. Rick, S. O'Neel, W. T. Pfeffer, R. S. Anderson, S. P. Anderson, and A. F. Glazovsky, 2007: Glaciers dominate eustatic sea-level rise in the 21st century. *Science,* **317,** 1064–1067.

Mesinger, F., and Coauthors, 2006: North American Regional Reanalysis. *Bull. Amer. Meteor. Soc.,* **87,** 343–360.

Otto-Bliesner, B. L., S. J. Marshall, J. T. Overpeck, G. H. Miller, and A. Hu, 2006a: Simulating arctic climate warmth and icefield retreat in the Last Interglaciation. *Science,* **311,** 1751–1753.

——, ——, ——, ——, and ——, 2006b: Support material: Simulating arctic climate warmth and icefield retreat in the Last Interglaciation. *Science,* **311,** 1751–1753.

Overland, J. E., and P. S. Guest, 1991: The Arctic snow and air temperature budget over sea ice during winter. *J. Geophys. Res.,* **96,** 4651–4662.

Raper, S. C. B., and R. J. Braithwaite, 2006: Low sea level rise projections from mountain glaciers and icecaps under global warming. *Nature,* **439,** 311–313.

Schuler, T. V., R. Hock, M. Jackson, H. Elvehoy, M. Braun, I. Brown, and J. O. Hagen, 2005: Distributed mass-balance and climate sensitivity modelling of Engabreen, Norway. *Ann. Glaciol.,* **42,** 395–401.

Serreze, M. C., and R. G. Barry, 2005: *The Arctic Climate System.* Cambridge Atmospheric and Space Science Series, Cambridge University Press, 385 pp.

——, J. D. Kahl, and R. C. Schnell, 1992: Low-level temperature inversions of the Eurasian Arctic and comparisons with Soviet drifting station data. *J. Climate,* **5,** 615–629.

Sharp, M., L. Copland, K. Filbert, D. Burgess, and S. Williamson, 2003: Recent changes in the extent and volume of Canadian Arctic glaciers. *Papers and Recommendations: Snow Watch 2002 Workshop and Workshop on Assessing Global Glacier Recession,* Glaciological Data Rep. GD-32, Boulder, CO, NSIDC, 73–75.

Shepherd, A., Z. Du, T. J. Benham, J. A. Dowdeswell, and E. M. Morris, 2007: Mass balance of Devon Ice Cap, Canadian Arctic. *Ann. Glaciol.,* **46,** 249–254.

Shumway, R. H., and D. S. Stoffer, 2006: *Time Series Analysis and Its Applications: With R Examples.* 2nd ed. Springer-Verlag, 575 pp.

Steffen, K., and J. Box, 2001: Surface climatology of the Greenland Ice Sheet: Greenland climate network 1995-1999. *J. Geophys. Res.,* **106,** 33 951–33 964.

——, S. V. Nghiem, R. Huff, and G. Neumann, 2004: The melt anomaly of 2002 on the Greenland Ice Sheet from active and passive microwave satellite observations. *Geophys. Res. Lett.,* **31,** L20402, doi:10.1029/2004GL020444.

Thomas, R. H., W. Abdalati, E. Frederick, W. B. Krabill, S. Manizade, and K. Steffen, 2003: Investigation of surface melting and dynamic thinning on Jakobshavn Isbrae, Greenland. *J. Glaciol.,* **49,** 231–239.

van den Broeke, M. R., 1997: Structure and diurnal, variation of the atmospheric boundary layer over a mid-latitude glacier in summer. *Bound.-Layer Meteor.,* **83,** 183–205.

von Storch, H., and F. W. Zwiers, 1999: *Statistical Analysis in Climate Research.* Cambridge University Press, 484 pp.

Wang, L., M. J. Sharp, B. Rivard, S. Marshall, and D. Burgess, 2005: Melt season duration on Canadian Arctic ice caps, 2000–2004. *Geophys. Res. Lett.,* **32,** L19502, doi:10.1029/2005GL023962.

Wright, A., J. Wadham, M. Siegert, A. Luckman, and J. Kohler, 2005: Modelling the impact of superimposed ice on the mass balance of an Arctic glacier under scenarios of future climate change. *Ann. Glaciol.,* **42,** 277–283.